

Relative rotation rates for driven dynamical systems

H. G. Solari and R. Gilmore

Department of Physics and Atmospheric Science, Drexel University, Philadelphia, Pennsylvania 19104

(Received 16 April 1987)

Relative rotation rates for two-dimensional driven dynamical systems are defined with respect to arbitrary pairs of periodic orbits. These indices describe the average rate, per period, at which one orbit rotates around another. These quantities are topological invariants of the dynamical system, but contain more physical information than the standard topological invariants for knots, the linking and self-linking numbers, to which they are closely related. This definition can also be extended to include noisy periodic orbits and strange attractors. A table of the relative rotation rates for a dynamical system, its intertwining matrix, can be used to determine whether orbit pairs can undergo bifurcation and, if so, the order in which the bifurcations can occur. The relative rotation rates are easily computed and measured. They have been computed for a simple model, the laser with modulated parameter. By comparing these indices with those of a zero-torsion lift of a horseshoe return map, we have been able to determine that the dynamics of the laser are governed by the formation of a horseshoe. Additional stable periodic orbits, besides the principal subharmonics previously reported, are predicted by the dynamics. The two additional period-five attractors have been located with the aid of their logical sequence names, and their identification has been confirmed by computing their relative rotation rates.

I. INTRODUCTION

The motivation for the present work is twofold: (1) to provide a deeper understanding of a particular physical system, the laser with modulated parameter, and (2) to develop methods useful for the description of other two-dimensional periodically driven damped dynamical systems. To this end we have introduced the concept of relative rotation rate and studied its properties.

The relative rotation rate describes the average rotation of one periodic orbit around another in a periodically forced nonlinear oscillator. This orbit-pair index is related to the linking number and self-linking numbers, which are topological indices describing pairs of periodic orbits or single periodic orbits.

Relative rotation rates are directly measurable in periodically driven physical systems. As a result, these topological indices are themselves directly accessible to physical measurement. Relative rotation rates impose three different kinds of constraints on dynamical systems.

(1) As a control parameter is varied, coexisting orbits may interact, typically through saddle-node or period-doubling bifurcations. The set of relative rotation rates provides "selection rules" on those bifurcations which are forbidden, those which are allowed, and the order in which allowed bifurcations can occur.

(2) The set of relative rotation rates provides information on whether two dynamical systems may be equivalent to each other or whether they are inequivalent.

(3) Relative rotation rates may suggest the mechanism responsible for creation of stable periodic orbits through saddle-node and period-doubling bifurcations. For example, these numbers may be fingerprints of a Smale horseshoe, as occurs in the present study.

Since this concept was introduced to help organize the

complexity present in the driven laser system, these complexities are surveyed in Sec. II. In Sec. III we introduce the relative rotation rates, illustrating both it and its implications in the context of the laser model. These ideas are applied to a more thorough discussion of the laser model in Sec. IV. Certain properties of the laser system suggest that the dynamics may be organized by a horseshoe map. The relative rotation rates are computed for the horseshoe in Sec. V. In Sec. VI the set of relative rotation rates for the horseshoe and laser model are compared. We close with a discussion of our results.

II. PROPERTIES OF A LASER WITH MODULATED PARAMETER

The equations of motion for a periodically driven two-dimensional dynamical system are

$$\begin{aligned} dx_i/dt &= f_i(x;t), \quad x \in R^2 \\ f_i(x;t) &= f_i(x;t+T). \end{aligned} \quad (1)$$

The forcing terms f_i have a minimum period T and typically depend on one or more control parameters. The phase space for such dynamical systems is $R^2 \times S^1$, where S^1 (the circle) parametrizes the time direction. Solutions of this system of equations may exhibit chaotic behavior since the phase space is sufficiently large.¹⁻³

A number of physical systems described by equations of type (1) have been studied. These include electric circuits,⁴⁻⁷ laser systems,⁸⁻¹⁹ a biological model,²⁰ a bouncing ball,²¹ etc. The behavior of each system is summarized by its bifurcation diagram. Although the bifurcation diagram for each system is distinct, they share more similarities than they exhibit differences. We are therefore encouraged to believe that methods developed to enhance the understanding of one such system will be

useful for all such systems.

To fix ideas, and for the sake of concreteness, we will focus our attention on the rate equations for a laser with modulated parameter. This system has been studied both experimentally⁸⁻¹⁴ and theoretically,^{15,16} with results that are in qualitative agreement. The rate equations for the laser intensity u and the population inversion z are

$$\begin{aligned} du/dt &= [z - R \cos(\Omega t)]u, \\ dz/dt &= (1 - \epsilon_1 z) - (1 + \epsilon_2 z)u, \end{aligned} \tag{2}$$

where ϵ_1, ϵ_2 are damping parameters, and R and Ω are the amplitude and frequency of the loss modulation term, respectively. The bifurcation diagram for this system is shown in Fig. 1 as a function of the single control parameter R for fixed values of the remaining control parameters.

The following features are particularly noteworthy.

Several different stable solutions can coexist for a given parameter value. These solutions are subharmonics of the fundamental, with periods nT , $n = 2, 3, 4, \dots$, or period doublings of the subharmonics. Subharmonics up to period 11 have been seen both experimentally and numerically. There is reason^{22,23} to believe that for any n , a (at least one) subharmonic exists, but that the rapidly decreasing size of the basin with increasing n makes the higher subharmonics increasingly difficult to detect.

All subharmonics ($n \geq 2$) are born in saddle-node bifurcations. These saddle-node bifurcations create a stable and a regular saddle orbit of period n (≥ 2). Every stable orbit born in a saddle-node bifurcation undergoes a period-doubling cascade. The cascade terminates in an accumulation point, with the usual Feigenbaum scaling.^{24,25} On the far side of the accumulation point there

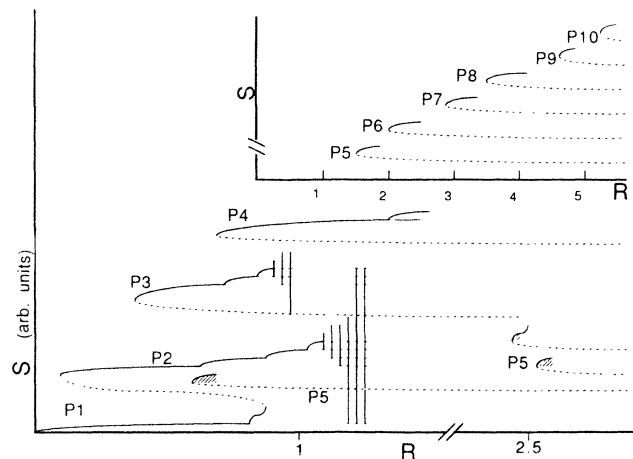


FIG. 1. Bifurcation diagram for the laser equations (2) shown as a function of the control parameter R . The periodicity of the various branches is shown (P1, P2, P3, . . .). Stable (—), regular saddle (---), and Möbius or flip saddle (· · ·) orbits are shown, as well as the strange attractors (|||) and crises. The two period-five orbits in the crosshatched regions are discussed in Sec. VI. Periodic orbits have been located with a standard numerical technique (Ref. 50). The parameter values for this diagram are $\epsilon_1 = 0.03$, $\epsilon_2 = 0.009$, $\Omega = 1.5$.

is a series of noisy periodic orbits which undergoes an inverse cascade.^{26,27} Feigenbaum scaling is obeyed in this region also. The ratio of the canonical scaling on both sides of the accumulation point, 0.18781. . ., appears to be obeyed.^{27,28} Beyond the last inverse bifurcation a strange attractor, based on the initial period n orbit, is formed.

The regular saddles created in the saddle-node bifurcations cannot undergo period doubling since the flow (2) is weakly contracting.²⁹ With the exception of the period-two regular saddle, all regular saddles exist to the right of the saddle-node bifurcation in which they are created.

We call the collection of orbits associated with a saddle-node bifurcation a branch. A branch consists of the regular period- n saddle, the initial period- n stable subharmonic, its stable progeny of period $n \times 2^k$ and the associated flip (Möbius) saddles, the noisy period $n \times 2^k$ orbits, and the “period- n ” strange attractor.¹⁶

Only the fundamental is not born in a saddle-node bifurcation. It undergoes an initial period-doubling bifurcation. The resulting stable period-two orbit is then annihilated in an inverse saddle-node bifurcation with the regular period-two saddle belonging to the period-two branch. The regular and flip saddles are involved in three kinds of crises.³⁰

(1) The flip saddles of period $n \times 2^k$ can collide with the boundary of a region of noisy periodicity $n \times 2^{k+1}$ to produce a noisy period-halving bifurcation. Such a collision is called an internal crisis.

(2) A regular saddle in a period- n branch can collide with the boundary of a “period- n ” strange attractor, thereby annihilating or enlarging it. Such a collision is called a boundary crisis.

(3) A regular saddle in a period n branch can collide with the boundary of a “period- n ” strange attractor ($n \neq n'$), thereby annihilating or enlarging it. Such a collision is called an external crisis.

These phenomena are summarized in Fig. 2. Since

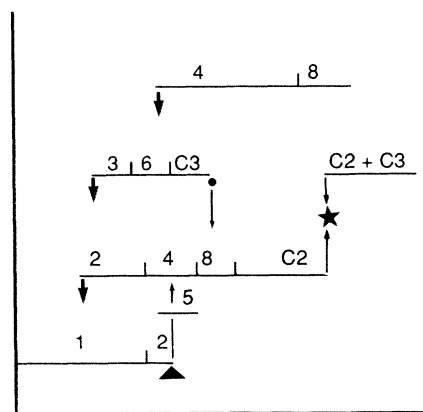


FIG. 2. A schematic is presented of the bifurcation diagram shown in Fig. 1. In this diagram (↓) indicates saddle node bifurcation, (▲) an inverse saddle-node bifurcation, (●) a boundary crisis, and (★) an external crisis. Here C2, C3 are the strange attractors based on the period-two and period-three branches.

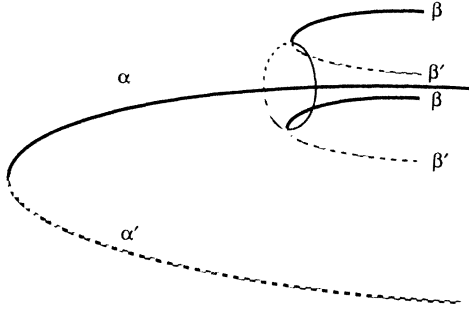


FIG. 3. The relative rotation rate is not a branch invariant. Here a saddle-node bifurcation creates the stable (—) and unstable (---) orbit pair α, α' . This is followed by another saddle-node bifurcation which creates the orbit pair β, β' which intertwines the stable orbit α but not α' .

four full rotations per eight periods.

This dependence on initial conditions may seem a bit awkward for a topological pair index. However, we will see below that a well-known topological index (linking number) can be constructed from the set of relative rotation rates for a pair of orbits. Thus, the orbit-pair relative rotation rates provide an even more refined diagnostic for orbital linking than the topological knot invariant.

(4) Self-rotation rate: The relative rotation rate can be defined for an orbit with itself, as $R_{ij}(A, A)$. The definition (3) is applicable, with $i \neq j$, as the integral (3) fails to be defined in this case. [Below, we will adopt the useful convention that $R_{ii}(A, A) = 0$.]

(5) Branch properties: The relative rotation rate is not a branch invariant. For example, a pair of orbits may be created in a saddle-node bifurcation (Fig. 3) which encircles just one periodic orbit of a branch pair. The two members of the original branch then have different relative rotation rates with respect to the new saddle-node pair. We will see below that the laser system (2) possesses additional period-five orbits, some of which (e.g., x^2y^3 in Table IV) wind around the stable period-one branch (y) and her daughter (xy) in different ways.

(6) The relative rotation rates between the two orbits created in a saddle-node bifurcation and all other orbits which exist at the time of the saddle-node bifurcation are the same. This is because the two orbits are localized arbitrarily closely at the time of their creation.

(7) Similarly, the relative rotation rates of all orbits ($n \times 2^k$, stable and Möbius) created in a cascade are unchanged with respect to all branches which exist

throughout the duration of the cascade, for the same localization reasons.

(8) The relative rotation rates for orbits within a branch, created during a cascade, are nontrivial. The relative rotation rates for the orbits involved in the period-one cascade for the laser system (2) are given in Table II. Tables for the other subharmonic branches are identical to this table, up to an overall multiplicative factor which is $1/n$ for the principal subharmonic branch of period nT (i.e., the orbits based on the fundamental with logical sequence $x^{n-1}y$, cf. Sec. V below).

(9) Saddle-node pairs: Orbits created in a saddle-node bifurcation have the same set of self-rotation rates. Their relative rotation rates are related to the self-rotation rates in a simple way. If the self-rotation rates are $(r_1, r_2, \dots, r_{p_A-1}, 0)^{p_A}$, the relative rotation rates are $(r_1, r_2, \dots, r_{p_A-1}, r_{p_A})^{p_A}$. The last ratio r_{p_A} describes the rotation of the flow around the orbit in the neighborhood of the closed orbit. This is related to the local torsion³¹⁻³⁵ [cf. Eq. (6) below].

(1) Mother-daughter pairs: Similar results hold for the unstable Möbius saddle of period p_A and its stable daughter of period $2p_A$ involved in a period-doubling bifurcation. If the self-rotation rates of the mother orbit are $(r_1, r_2, \dots, r_{p_A-1}, 0)^{p_A}$, the self-rotation rates of the daughter are $(r_1^2, r_2^2, \dots, r_{p_A-1}^2, r_{p_A}, 0)^{2p_A}$, and the relative rotation rates are $(r_1, r_2, \dots, r_{p_A-1}, r_{p_A})^{2p_A}$, with r_{p_A} as defined above. These results for saddle-node and mother-daughter pairs follow from the localization property during their bifurcation.

E. Uses

(1) The intertwining matrix provides selection rules on bifurcations. Two orbits cannot interact via bifurcation unless their relative rotation rates are identical with respect to all other existing orbits. Inspection of Table I shows that of the orbits listed which are not created in saddle-node bifurcations (Na and Nb), only the period-one [1 and 2(1)] and period-two ($2b$) orbits can interact. In addition, the two period-three orbits cannot interact while the period-doubled period-six [6(3)] orbit exists. The latter must first be absorbed by $3a$ (as a function of decreasing R) before $3a$ and $3b$ can interact in a saddle-node bifurcation. Similar remarks are valid for $2a$, $2b$, and $4(2)$, and more generally for cascades based on period

TABLE II. Relative rotation rates for the period-doubling cascade based on the period-one period-two branch. Instead of providing all $p_A \times p_B$ ratios, this table provides the ratios of occurrences of these rates. For period-doubling cascades based on a period- n orbit, the relative rotation rates of that orbit must be added to all matrix elements. This table is symmetric.

	1	2	4	8	16
1	0	$-\frac{1}{2}$	$-\frac{1}{2}$	$-\frac{1}{2}$	$-\frac{1}{2}$
2		$-\frac{1}{2}, 0$	$-\frac{1}{2}, -\frac{1}{4}$	$-\frac{1}{2}, -\frac{1}{4}$	$-\frac{1}{2}, -\frac{1}{4}$
4			$(-\frac{1}{2})^2, (-\frac{1}{4}), 0$	$(-\frac{1}{2})^2, -\frac{1}{4}, -\frac{3}{8}$	$(-\frac{1}{2})^2, -\frac{1}{4}, -\frac{3}{8}$
8				$(-\frac{1}{2})^4, (-\frac{1}{4})^2, -\frac{3}{8}, 0$	$(-\frac{1}{2})^4, (-\frac{1}{4})^2, -\frac{3}{8}, -\frac{5}{16}$
16					$(-\frac{1}{2})^8, (-\frac{1}{4})^4, (-\frac{3}{8})^2, -\frac{5}{16}, 0$

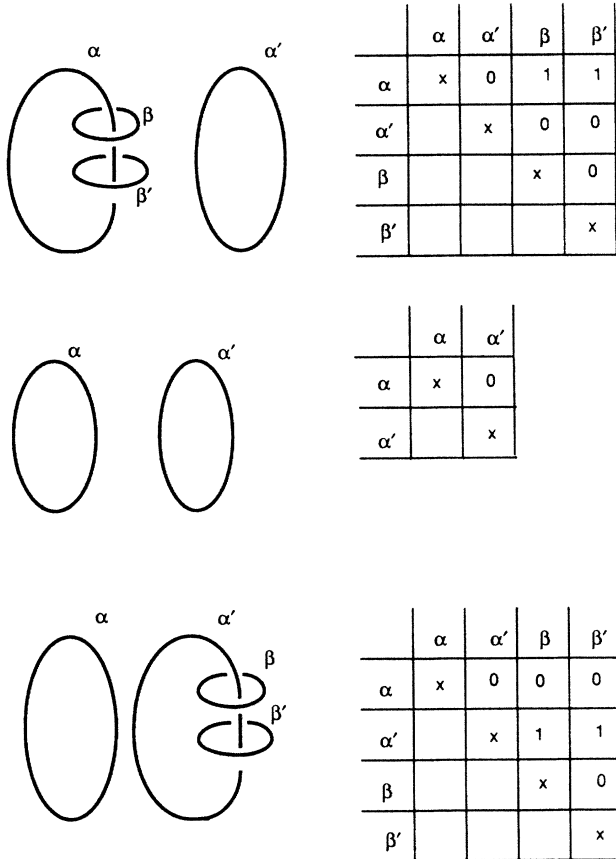


FIG. 4. The intertwining matrix contains information about the topological organization of the periodic orbits. It indicates whether orbits can interact through bifurcation, and the order in which the interactions can occur. Here α, α' cannot interact until β, β' disappear.

$N: Nb$ and $Na, 2 \times N(N), 2^2 \times N(N), \dots, 2^k \times N(N)$.

(2) The intertwining matrix can be used to predict the order in which bifurcations can occur. For example, two orbits (α, α' in Fig. 4) may not be able to interact because they are linked differently by other orbits (β, β'). The intervening orbits (β, β') must first be annihilated before the orbits (α, α') can coalesce by bifurcation. Creation or annihilation of orbits corresponds to adding or deleting the corresponding rows and columns to or from the intertwining matrix.

F. Extensions

The relative rotation rate has been defined for pairs of periodic orbits. This definition can be extended to include noisy periodic orbits or even aperiodic orbits. If A has period p_A and B has noisy period p_B , then the time integral over $p_A \times p_B$ periods is not quite an integer (Fig. 5). Similarly, the integral over $p_A \times p_B \times m$ periods ($m = 2, 3, 4, \dots$) is not an integer—it differs from an integer by an amount related to the “solid angle” of the noisy periodic region as seen from one of the periodic points. Therefore, the limit

$$R_{ij}(A, B) = \lim_{\tau \rightarrow \infty} \frac{T}{2\pi\tau} \int_{t_0}^{t_0+\tau} \frac{\mathbf{n} \cdot (\Delta \mathbf{r} \times d\Delta \mathbf{r})}{\Delta \mathbf{r} \cdot \Delta \mathbf{r}}, \quad (4)$$

where $\tau = p_A \times p_B \times m \times T$ and t_0 determines the Poincaré section, exists and determines the average rotation rate of the periodic orbit around a tube containing the noisy periodic orbit. Here i indexes an intersection a_i of A with a Poincaré section and j indexes a noisy periodic region of the orbit B in the Poincaré section. The integral is well defined as long as the periodic orbit is disjoint from the tube containing the noisy periodic orbit. This limit is a rational fraction which may be interpreted at the relative rotation rate of the period p_A orbit with any closed period p_B orbit embedded in the tube containing the noisy period p_B orbit. This definition can be extended to pairs of noisy periodic orbits as long as the tubes surrounding both remain disjoint.

The extension (4) to noisy periodic orbits has been particularly useful in locating the noisy period-halving bifurcations in the inverse cascade along any branch. These bifurcations are difficult to locate numerically, and especially experimentally. Such bifurcations are located by taking A as the Möbius orbit of period $n \times 2^k$ which initiates the internal crisis, and B the orbit of noisy period $n \times 2^{k+1}$ (Fig. 6). The limit (4) remains constant up to the crisis, after which its value begins to change.¹⁶

The relative rotation rate has also been computed for strange attractors formed after the last period-halving crisis along each branch. In this region, the relative rotation rates typically begin to change from their well-defined fractional values (Fig. 7). By computing the relative rotation rates for the strange attractor on the period- n branch and regular periodic saddles, it is possible to determine when crises will occur, the regular saddles responsible for the crisis, the type of crisis (boundary or external), and the consequences of the crisis. The crises identified in the bifurcation diagram for the laser

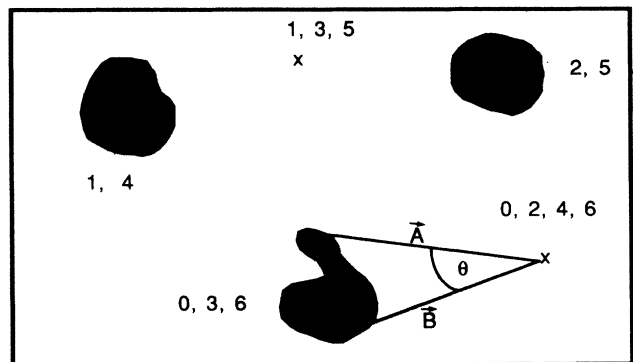


FIG. 5. The relative rotation rate is well defined, in the limit, between noisy periodic orbits and periodic orbits which do not intersect a tube containing the noisy periodic orbit. The difference vector \mathbf{A} between a point on a noisy period-three orbit and a period-two orbit evolves, after six periods, to the difference vector \mathbf{B} . The angle θ between the difference vectors \mathbf{A}, \mathbf{B} is bounded above by the solid angle subtended by a noisy period disk and a point on the periodic orbit. In the limit $T \rightarrow \infty$, the ratio (5) consists of the well-defined rational fractional part, and a stochastic part whose limit is zero.

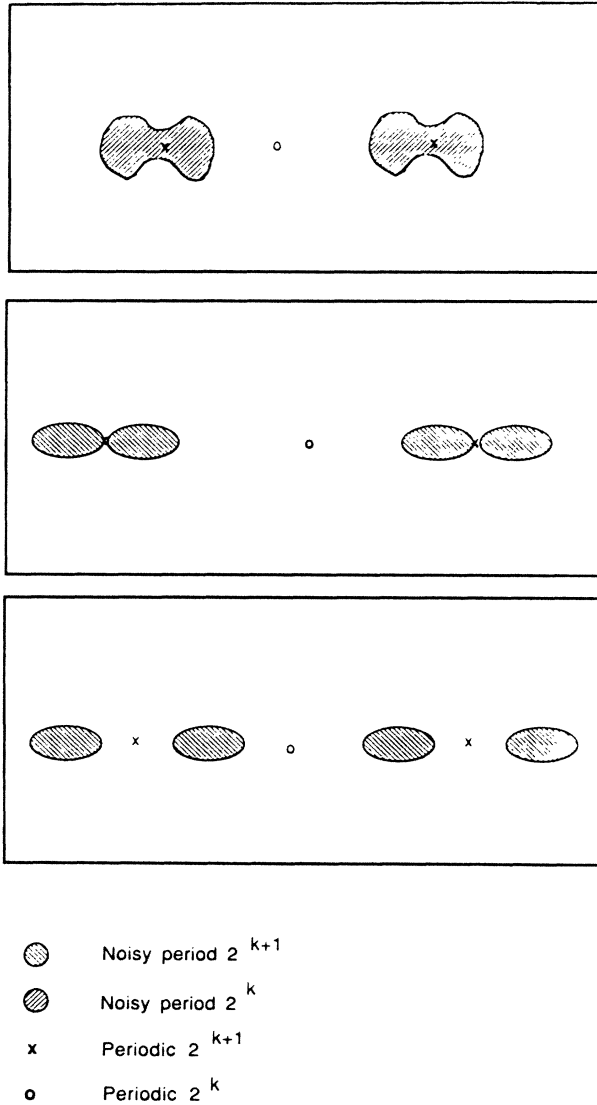


FIG. 6. Internal crises occur when the boundaries of noisy period 2^{k+1} regions collide with a period 2^k Möbius saddle.

(Figs. 1 and 2) were confirmed by computation of the appropriate relative rotation rates.

G. Mathematical extensions

The relative rotation rate depends on initial conditions, making the intertwining matrix somewhat awkward, as its matrix elements are not unique. There is a topological invariant, the knot linking number $L(A, B)$ which describes how two closed curves (periodic orbits) are linked or intertwined. The relative rotation rate and the linking number³⁶⁻³⁸ are simply related:

$$L(A, B) = \sum_{i,j} R_{ij}(A, B) . \tag{5}$$

A proof is presented in the Appendix. The matrix of linking numbers can be constructed directly from the intertwining matrix (not vice versa, with exceptions noted in Sec. V).

Every topological knot has a self-linking number^{31,32}

$L(A, A)$. It is therefore worthwhile to extend the relative-rotation-rate concept to the self rotation of a periodic orbit by identifying B with A in Eq. (2). The case $i = j$ must then be excluded, since the integral is undefined. In this way we are able to include the diagonal matrix elements in the intertwining matrix.

If by convention we define $L_{ii}(A, A) = 0$, then the definition (5) can be extended to include the self-linking number of an orbit with itself. The linking and self-linking numbers of some orbits of the laser system are given in Table III.

If the system dynamics are governed by a horseshoe, both the topological invariants $L(A, B)$ and dynamical invariants $R_{ij}(A, B)$ can be computed (Sec. V). The latter are measurable, so the former are also, by Eq. (4).

All results can be extended from nonautonomous two-dimensional dynamical systems to autonomous three-dimensional dynamical systems. It is only necessary to replace time as the integration parameter [in Eq. (3)] by a relative path length (an angle) along each orbit between successive intersections with the Poincaré section.

H. Practical results

(1) The relative rotation rates are directly accessible from physical data by triggering on the forcing terms.

(2) Many of the subharmonic branches are very localized in phase space. Even when they do not exist, no other orbits from other branches enter their characteristic region of phase space. It is then possible to compute the relative rotation rates even between orbits which do not simultaneously exist. For this reason it is possible to construct an intertwining matrix (Fig. 2) for orbits or branches which are non coexistent. In principle, this cannot always be done (Figs. 3 and 4), although in practice this has proved a valuable tool for study of the laser system.

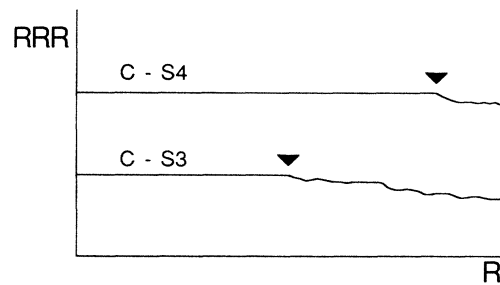


FIG. 7. The relative rotation rate (RRR) (C-S3) between the regular period-three saddle (S3) and the noisy periodic attractor on the period-one period-two branch (C) remains constant until the last internal crisis. This rate then begins to change. When the collision between the strange attractor and the regular period-three saddle occurs (external crisis), there is a sudden expansion of the strange attractor into the region of the stable period-three branch. Thereafter, the relative rotation rate between the regular period-three saddle and the period-one period-three strange attractor continues to change. The relative rotation rate (C-S4) between the chaotic attractor and the period-four regular saddle beings to change at a later crisis.

TABLE III. Linking numbers (off-diagonal) and self-linking numbers between low period orbits shown in Fig. 1. Notation is the same as in Table I.

	1	2a	2b	2(1)	4(2)	3a	3b	6(3)	4a	4b	5	6
1	0	1	1	1	2	1	1	2	1	1	1	1
2a	1	1	2	2	3	2	2	4	2	2	2	2
2b	1	2	1	2	4	2	2	4	2	2	2	2
2(1)	1	2	2	1	4	2	2	4	2	2	2	2
4(2)	2	3	4	4	5	4	4	8	4	4	4	4
3a	1	2	2	2	4	2	3	5	3	3	3	3
3b	1	2	2	2	4	3	2	6	3	3	3	3
6(3)	2	4	4	4	8	5	6	9	4	4	4	4
4a	1	2	2	2	4	3	3	4	3	4	4	4
4b	1	2	2	2	4	3	3	4	4	3	4	4
5	1	2	2	2	4	3	3	4	4	4	4	5
6	1	2	2	2	4	3	3	4	4	4	5	5

I. Comparison with previous work

Concepts related to the relative rotation rate have been discussed previously by a number of authors.

(1) Periodic orbits in the Lorenz system^{39,40} may rotate around the z axis (an invariant set). The number of rotations is an invariant. Two orbits with different rotation numbers cannot interact through saddle-node bifurcation, nor through period-doubling bifurcation unless their rotation numbers differ by a factor of 2.

(2) Parlitz and Lauterborn⁴¹ introduced a winding number defined as the number of maxima or minima of a projected periodic solution, per period. Although this is a useful index for particular dynamical systems, it is not a topological invariant. For the laser system (2), this index is initially different on the regular saddle of period-two and the period-doubled daughter on the period-one branch which undergo the inverse saddle-node bifurcation.

(3) The local torsion for the flow about a periodic orbit in a periodic-doubling cascade has been computed by Uezu.^{33,34} This is essentially the relative rotation rate of a mother-daughter pair of orbits, derivable from Eq. (3) and property (10) in Sec. III D above. Uezu has computed the local torsion and extracted the relation

$$T(k-1, k) = [(3m+2)2^{k-1} + (-1)^{k-1}] / 3 \quad (6)$$

between orbits of period 2^{k-1} and 2^k , where m is the crossing number of the fundamental. One of the relative rotation rates between a mother-daughter orbit pair is the local torsion divided by the period of the daughter orbit.

(4) Holmes^{42,43} has introduced the "putative braid index." This is simply the linking number between a period- n orbit and the (unique) period-one stable orbit or Möbius saddle in the system studied.

(5) Schmidt and Wang⁴⁴ have introduced a winding ratio (q/p) defined as the ratio of the number of rotations (q) which an orbit of period p makes around some invariant set, either a fixed point, a limit cycle, or a torus.

(6) The winding number q/p is defined as the number of rotations (q) a closed orbit (period p) makes on the surface of a torus. The corresponding knot is a torus knot of type (q, p) . This is essentially the linking number between the torus knot and the limit cycle from which

the torus bifurcated in a secondary Hopf bifurcation.

These definitions are all asymmetric, in that they do not treat arbitrary pairs of orbits on an equal footing. Since the only structurally stable elements which the dynamical system (1) possesses are the invariant sets, it is essential to use these elements in a symmetric way in order to characterize the flow properties of the system. The definition (3) does this.

IV. APPLICATION TO THE LASER

We illustrate the use of the intertwining matrix by applying it to the laser system (2). The intertwining matrix for this system is presented in Tables I and II. There are three period-two orbits: $2a$, $2b$, and $2(1)$. These coexist over a finite range of parameter values. Since the orbits $2b$ and $2(1)$ have identical sets of relative rotation rates with respect to all other orbits shown, it is possible for these two orbits to interact. This interaction is an inverse saddle-node bifurcation which occurs at $R=0.96$, destroying both orbits. The orbits $2a$ and $2b$ do not have identical sets of relative rotation rates with respect to all other orbits shown. Specifically, the relative rotation

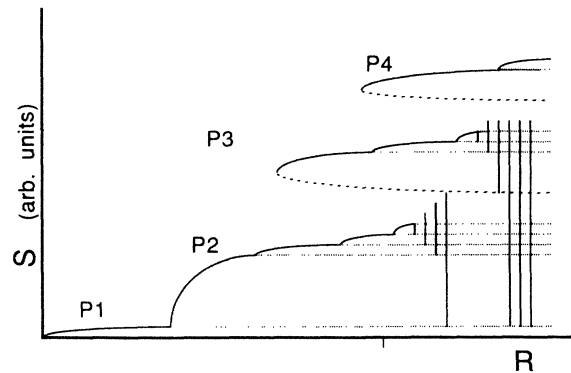


FIG. 8. A deformation of the laser system (2) can be found which "straightens out" the snake of the periodic-one branch. The orbits shown, as well as all the other orbits shown in Fig. 1, together with the two additional period-five branches, have relative rotation rates as predicted from the horseshoe map.

rates differ with respect to the orbit 4(2). Therefore, the two orbits $2a$ and $2b$ cannot interact while the orbit 4(2) exists. This, of course, is clear. The period-doubled orbit 4(2) must first interact with the orbit $2a$ (getting destroyed in a period-halving bifurcation as a function of decreasing R) before $2b$ can interact with $2a$ in an inverse saddle-node bifurcation which destroys them both.

The intertwining matrix shows that $2a$ and $2b$ can interact through a saddle-node bifurcation (R increasing) while $2b$ and $2(1)$ can interact through inverse saddle-node bifurcation. Thus we predict that we can deform the laser equation (i.e., by changing the values of the parameters $\epsilon_1, \epsilon_2, \Omega$) to eliminate both saddle-node bifurcations (Fig. 8) to "straighten out the snake." Such a deformation exists and has been found.

It is profitable to regard the period-two branch of the original laser system (Fig. 1) as simply a continuation of the period-one branch: $1-2(1)-2b-2a$. Such a continuation is called a "snake" by Yorke and co-workers.^{38,45,46} In this sense the laser system has no period-two branch. This can be made more precise by observing the spectrum of regular periodic saddles for sufficiently large control parameter values: regular saddles of periods 3,4,5, . . . created in saddle-node bifurcations persist for all larger values of R . There is also a single stable period-one orbit for small control parameter values as well as one regular period-one saddle for all values of R . In consequence, branches of periods 1,3,4,5, . . . are identifiable, but there is no period-two branch.

V. HORSESHOES

One difficulty of previous studies of driven damped dynamical systems has been the lack of information on the existence and multiplicity of subharmonic branches of any periodicity. For example, it would be useful to be able to make statements of the form "For any n there is a subharmonic branch" or "For any n there are (no more than) $N(n)$ subharmonic branches." These are analogous to completeness statements of linear systems theory. The only mechanisms available for providing completeness statements are mapping constructions of horseshoe-type.⁴⁷ The presence of a horseshoe is suggested by the partial spectrum of regular periodic saddles, and particularly the absence of a regular period-two saddle.

To test this possibility, we investigated the return map of the outset of the regular period-one saddle which exists for all R values. This return, for large R values, indicated the incomplete formation of a horseshoe. This information suggested that it would be useful to compute the relative rotation rate for the horseshoe return map.

There is, of course, the difficulty that the horseshoe is a map while the construction of relative rotation rates must be carried out for flows. The fitting of a horseshoe return map to a flow is unique up to an overall rotation (torsion) about the axis of the flow. Figure 9(a) shows a lift of the horseshoe map to a flow with zero torsion; Fig. 9(b) shows a lift with torsion +1.

It is now possible to compute the intertwining matrix for any flow whose underlying return map is a horseshoe. First, the torsion of the lift is computed. This may be

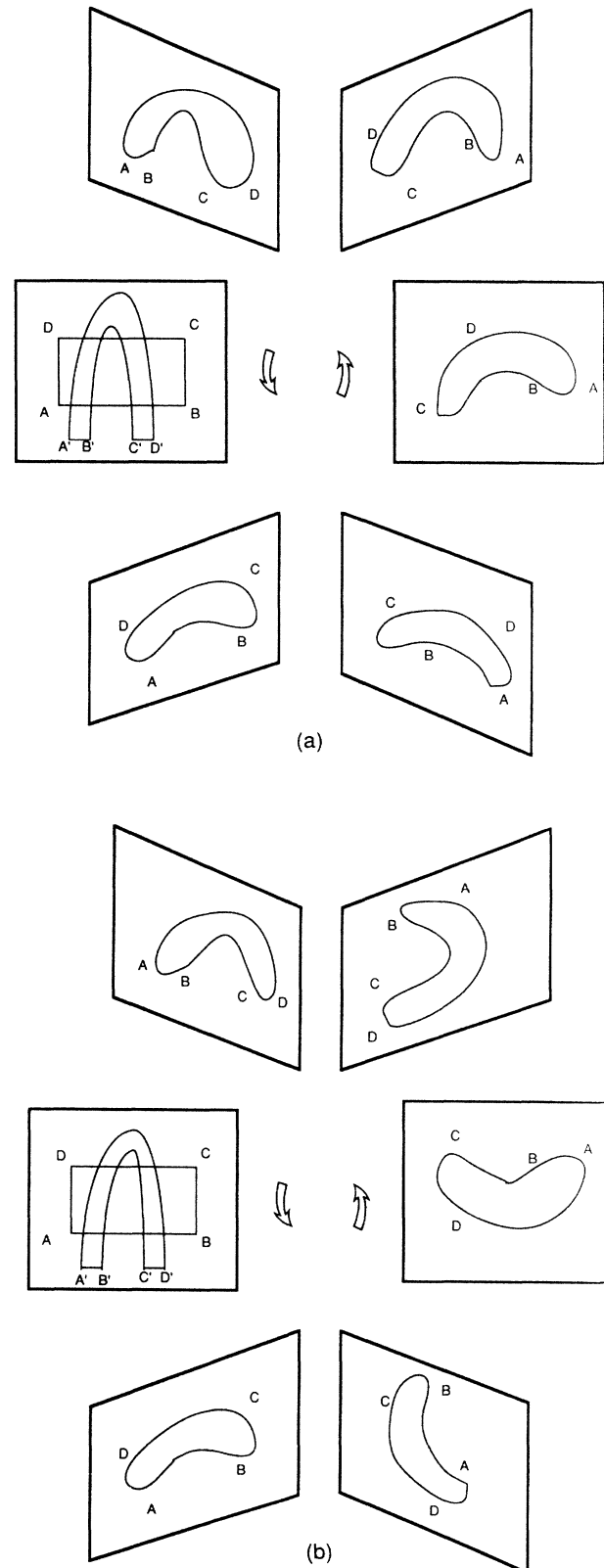


FIG. 9. (a) A zero-torsion lift of the horseshoe return map has intersections with the planes "phase=constant" as shown. (b) This lift of the horseshoe map to a flow has torsion +1; one complete clockwise rotation (as seen looking into the flow) of the image on the plane "phase=constant" is made per period.

TABLE IV. Relative rotation rates for the zero-torsion lift of the horseshoe. All rotation rates are clockwise; the negative sign has not been shown. This table shows the relative number of occurrences when two or more ratios occur by varying the initial conditions. Orbits are named by their logical sequence; the corresponding orbit for the laser system is indicated in the second column. Parentheses after period indicates the R value at which orbit is created by saddle-node bifurcation. Notation is as in Table I: a , stable; b , regular saddle; 2(1) and 6(3) are period-doubled orbits along period-one and period-three branches. T indicates torsion of the horseshoe lift. This is the relative rotation rate of the two period-one orbits about each other. If this is nonzero, the positive or negative integer T should be added to all entries in this matrix (which are nonpositive).

		x	y	xy	x^2y	xy^2	x^3y	x^2y^2	x^4y	x^3y^2	x^2y^3	x^2yxy	xy^4
x	1b	0	T	0	0	0	0	0	0	0	0	0	0
y	1a	T	0	$\frac{1}{2}$	$\frac{1}{3}$	$\frac{1}{3}$	$\frac{1}{4}$	$\frac{1}{4}$	$\frac{1}{5}$	$\frac{1}{5}$	$\frac{2}{5}$	$\frac{2}{5}$	$\frac{2}{5}$
xy	2(1)	0	$\frac{1}{2}$	$\frac{1}{2}, 0$	$\frac{1}{3}$	$\frac{1}{3}$	$\frac{1}{4}$	$\frac{1}{4}$	$\frac{1}{5}$	$\frac{1}{5}$	$\frac{3}{10}$	$\frac{3}{10}$	$\frac{2}{5}$
x^2y	3a	0	$\frac{1}{3}$	$\frac{1}{3}$	$(\frac{1}{3})^2, 0$	$\frac{1}{3}$	$\frac{1}{4}$	$\frac{1}{4}$	$\frac{1}{5}$	$\frac{1}{5}$	$\frac{4}{15}$	$\frac{4}{15}$	$\frac{1}{3}$
xy^2	3b	0	$\frac{1}{3}$	$\frac{1}{3}$	$\frac{1}{3}$	$(\frac{1}{3})^2, 0$	$\frac{1}{4}$	$\frac{1}{4}$	$\frac{1}{5}$	$\frac{1}{5}$	$\frac{1}{3}$	$\frac{1}{3}$	$\frac{1}{3}$
x^3y	4a	0	$\frac{1}{4}$	$\frac{1}{4}$	$\frac{1}{4}$	$\frac{1}{4}$	$(\frac{1}{4})^3, 0$	$\frac{1}{4}$	$\frac{1}{5}$	$\frac{1}{5}$	$\frac{1}{4}$	$\frac{1}{4}$	$\frac{1}{4}$
x^2y^2	4b	0	$\frac{1}{4}$	$\frac{1}{4}$	$\frac{1}{4}$	$\frac{1}{4}$	$\frac{1}{4}$	$(\frac{1}{4})^3, 0$	$\frac{1}{5}$	$\frac{1}{5}$	$\frac{1}{4}$	$\frac{1}{4}$	$\frac{1}{4}$
x^4y	5a (1.40)	0	$\frac{1}{5}$	$\frac{1}{5}$	$\frac{1}{5}$	$\frac{1}{5}$	$\frac{1}{5}$	$\frac{1}{5}$	$(\frac{1}{5})^4, 0$	$\frac{1}{5}$	$\frac{1}{5}$	$\frac{1}{5}$	$\frac{1}{5}$
x^3y^2	5b (1.40)	0	$\frac{1}{5}$	$\frac{1}{5}$	$\frac{1}{5}$	$\frac{1}{5}$	$\frac{1}{4}$	$\frac{1}{5}$	$\frac{1}{5}$	$(\frac{1}{5})^4, 0$	$\frac{1}{5}$	$\frac{1}{5}$	$\frac{1}{5}$
x^2y^3	5a (2.66)	0	$\frac{2}{5}$	$\frac{3}{10}$	$\frac{4}{15}$	$\frac{1}{3}$	$\frac{1}{5}$	$\frac{1}{4}$	$\frac{1}{5}$	$\frac{1}{5}$	$(\frac{1}{5})^2, (\frac{2}{5})^2, 0$	$(\frac{1}{5})^3, (\frac{2}{5})^2$	$(\frac{1}{5}), (\frac{2}{5})^4$
x^2yxy	5b (2.66)	0	$\frac{2}{5}$	$\frac{3}{10}$	$\frac{4}{15}$	$\frac{1}{3}$	$\frac{1}{5}$	$\frac{1}{4}$	$\frac{1}{5}$	$\frac{1}{5}$	$(\frac{1}{5})^3, (\frac{2}{5})^2$	$(\frac{1}{5})^2, (\frac{2}{5})^2, 0$	$(\frac{1}{5}), (\frac{2}{5})^4$
xy^4	5b (0.80)	0	$\frac{2}{5}$	$\frac{2}{5}$	$\frac{1}{3}$	$\frac{1}{3}$	$\frac{1}{4}$	$\frac{1}{4}$	$\frac{1}{5}$	$\frac{1}{5}$	$(\frac{1}{5}), (\frac{2}{5})^4$	$(\frac{1}{5}), (\frac{2}{5})^4$	$(\frac{2}{5})^4, 0$
xy^2xy	5a (0.80)	0	$\frac{2}{5}$	$\frac{2}{5}$	$\frac{1}{3}$	$\frac{1}{3}$	$\frac{1}{4}$	$\frac{1}{4}$	$\frac{1}{5}$	$\frac{1}{5}$	$(\frac{1}{5})^2, (\frac{2}{5})^3$	$(\frac{1}{5})^2, (\frac{2}{5})^3$	$\frac{2}{5}$
x^2yxy^2	6(3)	0	$\frac{1}{3}$	$\frac{1}{3}$	$\frac{1}{6}, (\frac{1}{3})^2$	$\frac{1}{6}$	$\frac{1}{4}$	$\frac{1}{4}$	$\frac{1}{5}$	$\frac{1}{5}$	$\frac{3}{10}$	$\frac{3}{10}$	$\frac{1}{3}$
xy^5	6a	0	$\frac{1}{2}$	$\frac{1}{3}, \frac{1}{2}$	$\frac{1}{3}$	$\frac{1}{3}$	$\frac{1}{4}$	$\frac{1}{4}$	$\frac{1}{5}$	$\frac{1}{5}$	$\frac{11}{30}$	$\frac{11}{30}$	$\frac{2}{5}$
xy^3xy	6b	0	$\frac{1}{2}$	$\frac{1}{3}, \frac{1}{2}$	$\frac{1}{3}$	$\frac{1}{3}$	$\frac{1}{4}$	$\frac{1}{4}$	$\frac{1}{5}$	$\frac{1}{5}$	$\frac{1}{3}$	$\frac{1}{3}$	$\frac{2}{5}$
x^2y^4	6b	0	$\frac{1}{3}$	$\frac{1}{3}$	$\frac{1}{6}, (\frac{1}{3})^2$	$\frac{1}{3}$	$\frac{1}{4}$	$\frac{1}{4}$	$\frac{1}{5}$	$\frac{1}{5}$	$\frac{3}{10}$	$\frac{3}{10}$	$\frac{1}{3}$
x^2y^2xy	6a	0	$\frac{1}{3}$	$\frac{1}{3}$	$\frac{1}{6}, (\frac{1}{3})^2$	$\frac{1}{3}$	$\frac{1}{4}$	$\frac{1}{4}$	$\frac{1}{5}$	$\frac{1}{5}$	$\frac{3}{10}$	$\frac{3}{10}$	$\frac{1}{3}$
x^3y^3	6a	0	$\frac{1}{3}$	$\frac{1}{6}, \frac{1}{3}$	$\frac{1}{3}, (\frac{1}{6})^2$	$(\frac{1}{3})^2, \frac{1}{6}$	$\frac{1}{4}, \frac{1}{6}$	$\frac{1}{4}$	$\frac{1}{5}$	$\frac{1}{5}$	$\frac{4}{15}$	$\frac{7}{30}$	$\frac{3}{10}$
x^3yxy	6b	0	$\frac{1}{3}$	$\frac{1}{6}, \frac{1}{3}$	$\frac{1}{3}, (\frac{1}{6})^2$	$(\frac{1}{3})^2, \frac{1}{6}$	$\frac{1}{4}, \frac{1}{6}$	$\frac{1}{4}$	$\frac{1}{5}$	$\frac{1}{5}$	$\frac{4}{15}$	$\frac{7}{30}$	$\frac{3}{10}$
x^4y^2	6b (2.00)	0	$\frac{1}{6}$	$\frac{1}{6}$	$\frac{1}{6}$	$\frac{1}{6}$	$\frac{1}{6}$	$\frac{1}{6}$	$\frac{1}{6}$	$\frac{1}{6}$	$\frac{1}{6}$	$\frac{1}{6}$	$\frac{1}{6}$
x^5y	6a (2.00)	0	$\frac{1}{6}$	$\frac{1}{6}$	$\frac{1}{6}$	$\frac{1}{6}$	$\frac{1}{6}$	$\frac{1}{6}$	$\frac{1}{6}$	$\frac{1}{6}$	$\frac{1}{6}$	$\frac{1}{6}$	$\frac{1}{6}$

determined by computing the relative rotation rate of the two period-one orbits around each other.

Second, this torsion is added to each matrix element of a canonical intertwining matrix for the torsion-free lift. To construct this canonical matrix, the periodic orbits must be enumerated. This can be done using logical sequences.^{3,48} Once the rows and columns (periodic orbits) have been enumerated, the relative rotation rates can be computed. We have carried out these computations; the results are summarized in Table IV. These results were computed in two different ways: from kneading theory applied to one-dimensional maps with a single maximum (Holmes's template construction⁴³) and from a piecewise linear horseshoe.

A matrix of topological invariants, the linking and self-linking numbers, can be constructed from the intertwining matrix. This is presented in Table V. This matrix is constructed for the torsion-free lift. For lifts with torsion n the integer $p_A \times p_B \times n$ must be added to each matrix element: $L_n(A, B) = L_0(A, B) + p_A \times p_B \times n$. Tables VI and VII provide the relative rotation rates and

the linking and self-linking numbers for the period-doubling cascade based on the period-one branch.

Tables of relative rotation rates for cascades based on any periodic orbit can be constructed relatively easily. We first note that in a period-doubling bifurcation the daughter orbit rotates around the mother orbit. In the next period-doubling bifurcation the granddaughter winds around the daughter, and both together rotate around the mother orbit in the same way. Therefore the intertwining matrix becomes essentially trivial except along the major diagonal and the diagonals adjacent to it, which describe mother-daughter linking. The self-rotation and relative rotation rates for a mother-daughter pair, given in Sec. III D property (10) are summarized in Table VIII(a). Here the mother orbit has period p_A and the daughter $2p_A$. The additional relative rotation rate r_{p_A} , is the local torsion (6), divided by the period of the daughter orbit (local relative torsion). The intertwining matrix for cascades in the zero-torsion lift can be built up from the sequence of local torsions together with the rela-

TABLE IV. (Continued).

		xy^2xy	x^2yxy^2	xy^5	xy^3xy	x^2y^4	x^2y^2xy	x^3y^3	x^3yxy	x^4y^2	x^5y
x	1b	0	0	0	0	0	0	0	0	0	0
y	1a	$\frac{2}{5}$	$\frac{1}{3}$	$\frac{1}{2}$	$\frac{1}{2}$	$\frac{1}{3}$	$\frac{1}{3}$	$\frac{1}{3}$	$\frac{1}{3}$	$\frac{1}{6}$	$\frac{1}{6}$
xy	2(1)	$\frac{2}{5}$	$\frac{1}{3}$	$\frac{1}{3}, \frac{1}{2}$	$\frac{1}{3}, \frac{1}{2}$	$\frac{1}{3}$	$\frac{1}{3}$	$\frac{1}{3}, \frac{1}{6}$	$\frac{1}{3}, \frac{1}{6}$	$\frac{1}{6}$	$\frac{1}{6}$
x^2y	3a	$\frac{1}{3}$	$(\frac{1}{6}), (\frac{1}{3})^2$	$\frac{1}{3}$	$\frac{1}{3}$	$\frac{1}{6}, (\frac{1}{3})^2$	$\frac{1}{6}, (\frac{1}{3})^2$	$\frac{1}{3}, (\frac{1}{6})^2$	$\frac{1}{3}, (\frac{1}{6})^2$	$\frac{1}{6}$	$\frac{1}{6}$
xy^2	3b	$\frac{1}{3}$	$\frac{1}{6}$	$\frac{1}{3}$	$\frac{1}{3}$	$\frac{1}{3}$	$\frac{1}{3}$	$(\frac{1}{3})^2, \frac{1}{6}$	$(\frac{1}{3})^2, \frac{1}{6}$	$\frac{1}{6}$	$\frac{1}{6}$
x^3y	4a	$\frac{1}{4}$	$\frac{1}{4}$	$\frac{1}{4}$	$\frac{1}{4}$	$\frac{1}{4}$	$\frac{1}{4}$	$\frac{1}{4}, \frac{1}{6}$	$\frac{1}{4}, \frac{1}{6}$	$\frac{1}{6}$	$\frac{1}{6}$
x^2y^2	4b	$\frac{1}{4}$	$\frac{1}{4}$	$\frac{1}{4}$	$\frac{1}{4}$	$\frac{1}{4}$	$\frac{1}{4}$	$\frac{1}{4}$	$\frac{1}{4}$	$\frac{1}{6}$	$\frac{1}{6}$
x^4y	5a (1.40)	$\frac{1}{5}$	$\frac{1}{5}$	$\frac{1}{5}$	$\frac{1}{5}$	$\frac{1}{5}$	$\frac{1}{5}$	$\frac{1}{5}$	$\frac{1}{5}$	$\frac{1}{6}$	$\frac{1}{6}$
x^3y^2	5b (1.40)	$\frac{1}{5}$	$\frac{1}{5}$	$\frac{1}{5}$	$\frac{1}{5}$	$\frac{1}{5}$	$\frac{1}{5}$	$\frac{1}{5}$	$\frac{1}{5}$	$\frac{1}{6}$	$\frac{1}{6}$
x^2y^3	5a (2.66)	$(\frac{1}{5})^2, (\frac{2}{5})^3$	$\frac{3}{10}$	$\frac{11}{30}$	$\frac{1}{3}$	$\frac{3}{10}$	$\frac{3}{10}$	$\frac{4}{15}$	$\frac{4}{15}$	$\frac{1}{6}$	$\frac{1}{6}$
x^2yxy	5b (2.66)	$(\frac{1}{5})^2, (\frac{2}{5})^3$	$\frac{3}{10}$	$\frac{11}{30}$	$\frac{1}{3}$	$\frac{3}{10}$	$\frac{3}{10}$	$\frac{7}{30}$	$\frac{7}{30}$	$\frac{1}{6}$	$\frac{1}{6}$
xy^4	5b (0.80)	$\frac{2}{5}$	$\frac{1}{3}$	$\frac{2}{5}$	$\frac{2}{5}$	$\frac{1}{3}$	$\frac{1}{3}$	$\frac{3}{10}$	$\frac{3}{10}$	$\frac{1}{6}$	$\frac{1}{6}$
xy^2xy	5a (0.80)	$(\frac{2}{5})^4, 0$	$\frac{1}{3}$	$\frac{2}{5}$	$\frac{2}{5}$	$\frac{1}{3}$	$\frac{1}{3}$	$\frac{4}{15}$	$\frac{4}{15}$	$\frac{1}{6}$	$\frac{1}{6}$
x^2yxy^2	6(3)	$\frac{1}{3}$	$(\frac{1}{3})^4, (\frac{1}{6}), 0$	$\frac{1}{3}$	$\frac{1}{3}$	$(\frac{1}{3})^5, \frac{1}{6}$	$(\frac{1}{3})^5, \frac{1}{6}$	$\frac{1}{3}, \frac{1}{6}$	$\frac{1}{3}, \frac{1}{6}$	$\frac{1}{6}$	$\frac{1}{6}$
xy^5	6a	$\frac{2}{5}$	$\frac{1}{3}$	$(\frac{1}{3})^2, (\frac{1}{2})^3, 0$	$\frac{1}{3}, \frac{1}{2}$	$\frac{1}{3}$	$\frac{1}{3}$	$(\frac{1}{3})^5, \frac{1}{6}$	$(\frac{1}{3})^5, \frac{1}{6}$	$\frac{1}{6}$	$\frac{1}{6}$
xy^3xy	6b	$\frac{2}{5}$	$\frac{1}{3}$	$\frac{1}{3}, \frac{1}{2}$	$(\frac{1}{3})^2, (\frac{1}{2})^3, 0$	$\frac{1}{3}$	$\frac{1}{3}$	$(\frac{1}{3})^2, \frac{1}{6}$	$(\frac{1}{3})^2, \frac{1}{6}$	$\frac{1}{6}$	$\frac{1}{6}$
x^2y^4	6b	$\frac{1}{3}$	$(\frac{1}{3})^5, (\frac{1}{6})$	$\frac{1}{3}$	$\frac{1}{3}$	$(\frac{1}{3})^4, \frac{1}{6}, 0$	$(\frac{1}{3})^2, \frac{1}{6}$	$(\frac{1}{3})^2, \frac{1}{6}$	$(\frac{1}{3})^2, \frac{1}{6}$	$\frac{1}{6}$	$\frac{1}{6}$
x^2y^2xy	6a	$\frac{1}{3}$	$(\frac{1}{3})^5, (\frac{1}{6})$	$\frac{1}{3}$	$\frac{1}{3}$	$(\frac{1}{3})^2, \frac{1}{6}$	$(\frac{1}{3})^4, \frac{1}{6}, 0$	$\frac{1}{3}, \frac{1}{6}$	$\frac{1}{3}, \frac{1}{6}$	$\frac{1}{6}$	$\frac{1}{6}$
x^3y^3	6a	$\frac{4}{15}$	$\frac{1}{3}, \frac{1}{6}$	$(\frac{1}{3})^5, (\frac{1}{6})$	$(\frac{1}{3})^4, (\frac{1}{6})^2$	$\frac{1}{6}, (\frac{1}{3})^2$	$\frac{1}{3}, \frac{1}{6}$	$(\frac{1}{6})^3, (\frac{1}{3})^2, 0$	$\frac{1}{3}, (\frac{1}{6})^2$	$\frac{1}{6}$	$\frac{1}{6}$
x^3yxy	6b	$\frac{4}{15}$	$\frac{1}{3}, \frac{1}{6}$	$(\frac{1}{3})^5, (\frac{1}{6})$	$(\frac{1}{3})^4, (\frac{1}{6})^2$	$\frac{1}{6}, (\frac{1}{3})^2$	$\frac{1}{6}, \frac{1}{3}$	$\frac{1}{3}, (\frac{1}{6})^2$	$(\frac{1}{6})^3, (\frac{1}{3})^2, 0$	$\frac{1}{6}$	$\frac{1}{6}$
x^4y^2	6b (2.00)	$\frac{1}{6}$	$\frac{1}{6}$	$\frac{1}{6}$	$\frac{1}{6}$	$\frac{1}{6}$	$\frac{1}{6}$	$\frac{1}{6}$	$\frac{1}{6}$	$(\frac{1}{6})^5, 0$	$\frac{1}{6}$
x^5y	6a (2.00)	$\frac{1}{6}$	$\frac{1}{6}$	$\frac{1}{6}$	$\frac{1}{6}$	$\frac{1}{6}$	$\frac{1}{6}$	$\frac{1}{6}$	$\frac{1}{6}$	$\frac{1}{6}$	$(\frac{1}{6})^5, 0$

TABLE V. Linking and self-linking numbers for low period orbits of the zero-torsion lift of the horseshoe map.

	x	y	xy	x^2y	xy^2	x^3y	x^2y^2	x^4y	x^3y^2	x^2y^3	x^2yxy	xy^4	xy^2xy
x	0												
y	0	0											
xy	0	1	1										
x^2y	0	1	2	2									
xy^2	0	1	2	3	2								
x^3y	0	1	2	3	3	3							
x^2y^2	0	1	2	3	3	4	3						
x^4y	0	1	2	3	3	4	4	4					
x^3y^2	0	1	2	3	3	4	4	5	4				
x^2y^3	0	2	3	4	5	5	5	5	5	6			
x^2yxy	0	2	3	4	5	5	5	5	5	7	6		
xy^4	0	2	4	5	5	5	5	5	5	9	9	8	
xy^2xy	0	2	4	5	5	5	5	5	5	8	8	10	8

TABLE VI. Intertwining matrix for the cascade based on the period-one branch, assuming a zero-torsion lift. The relative rotation rates are the relative local torsions. The entries give only the relative occurrence of these rates. Scaling appropriately, the period-eight and period-16 orbits have the following spectrum of relative rotation rates: $64(\frac{1}{2}), 32(\frac{1}{4}), 16(\frac{3}{8}), 16(\frac{5}{16})$. $t_1 = \frac{1}{2}, t_2 = \frac{1}{4}, t_3 = \frac{3}{8}, t_4 = \frac{5}{16}$, etc.

k		0	1	2	3	4
	period	1	2	4	8	16
0	1	0	t_1	t_1	t_1	t_1
1	2	t_1	$t_1 0$	$t_1 t_2$	$t_1 t_2$	$t_1 t_2$
2	4	t_1	$t_1 t_2$	$t_1^2 t_2 0$	$t_1^2 t_2 t_3$	$t_1^2 t_2 t_3$
3	8	t_1	$t_1 t_2$	$t_1^2 t_2 t_3$	$t_1^4 t_2^2 t_3 0$	$t_1^4 t_2^2 t_3 t_4$
4	16	t_1	$t_1 t_2$	$t_1^2 t_2 t_3$	$t_1^4 t_2^2 t_3 t_4$	$t_1^8 t_2^4 t_3^2 t_4 0$

tive rotation rates of the fundamental orbit.

If the fundamental orbit along a branch has period p and self-rotation rates $(r_1, r_2, \dots, r_{p-1}, 0)^p$ with local relative torsions t_{k+1} around the orbits of period $p \times 2^k$,

$$I(k, k) = [2^k(r_1, r_2, \dots, r_{p-1}), 2^{k-1}(t_1), 2^{k-2}(t_2), \dots, 2^0(t_k), 0]^{p \times 2^k},$$

$$I(k, k+1) = [2^k(r_1, r_2, \dots, r_{p-1}), 2^{k-1}(t_1), 2^{k-2}(t_2), \dots, t_k, t_{k+1}]^{p \times 2^{k+1}}, \tag{7}$$

$$I(k, l) = [r_1, r_2, \dots, r_{p-1}, t_1, t_2, \dots, t_k, t_{k+1}]^{p \times 2^{k+l}}.$$

The local torsions are computed from (6), and the local relative torsions are

$$t_{k+1} = T(k, k+1) / p \times 2^{k+1}. \tag{8}$$

The integer m in Eq. (6) is the (local torsion -1) of the fundamental orbit. The local torsion obeys the equation of Fibonacci-type

$$T(k, k+1) = T(k-1, k) + 2 \times T(k-2, k-1), \tag{9}$$

with initial conditions $T(-1, 0) = 0, T(0, 1) = m - 1$. For the cascade along the period-one branch, the local torsions $T(0, 1), T(1, 2)$, etc. are 1, 1, 3, 5, 11, 21, 43, etc., and the local relative torsions $t_1, t_2, t_3, t_4, t_5, \dots$ are $1/2, 1/2^2, 3/2^2, 5/2^4, 11/2^5, 21/2^6$, etc.

The linking and self-linking numbers for any cascade are easily obtained from eq. (5). We note, first of all, that those far from the diagonal are simply related to the mother-daughter linking numbers, since all (great) granddaughters rotate around the mother in the same way as the daughter,

$$L(k, l) = 2^{l-(k+1)} L(k, k+1) \quad (l > k). \tag{10}$$

The linking and self-linking numbers are recursively related by [Table VIII(b)]

TABLE VII. Linking and self-linking numbers for the period-doubling cascade based on the period-one branch.

k		0	1	2	3	4	5
	period	1	2	4	8	16	32
0	1	0	1	2	4	8	16
1	2	1	1	3	6	12	24
2	4	2	3	5	13	26	52
3	8	4	6	13	23	51	102
4	16	8	12	26	51	97	205
5	32	16	24	52	102	205	399

then the matrix elements $I(k, l)$ of the intertwining matrix, describing the orbits of periods $p \times 2^k$ and $p \times 2^l$ ($k \leq l = 0, 1, 2, \dots$) are

$$S(k+1, k+1) = 4 \times S(k, k) + T(k, k+1), \tag{11}$$

$$L(k, k+1) = 2 \times S(k, k) + T(k, k+1).$$

The initial condition for this recursion relation is $S(0, 0) = p \times \sum r_i$. For the cascade along the period-one branch, the self-linking numbers are 0, 1, 5, 23, 97, 399, 1617, 6511, etc.

VI. SECOND APPLICATION TO THE LASER

The intertwining matrix for the zero-torsion lift of the horseshoe (Table IV) can be compared with the intertwining matrix of the laser after the three period-two orbits in the period-one snake have been identified, and two are removed from Table I. After this identification, the two intertwining matrices are equivalent for the orbits appearing in both. The observed period- n subharmonic in the physical system corresponds to the periodic orbit with logical sequence $x^{n-1}y$. This corresponds to both observation and intuition: in the laser the subharmonic orbits show one energetic spike and $n-1$ following tiny tremors. This is also expected on the basis of energy balance arguments.

The horseshoe scenario predicts additional subharmonic branches. The lowest subharmonic for which there is degeneracy is $n=5$, for which up to two additional branches could exist. For the subharmonics of period 6, 7, 8, 9, . . . , the maximum degeneracy of stable branches is 4, 9, 14, 28, Since the horseshoe is incomplete, not all branches will necessarily exist for any value of the control parameter. They all will exist if there is a complete horseshoe.

Location of another period- n subharmonic would provide a strong indication that the dynamics of the laser system is in fact governed by a horseshoe. Since basins decrease rapidly in size with increasing n and $n=5$ is the first periodicity with degenerate multiplicity, we searched

TABLE VIII. (a) Elements of the intertwining matrix $I(k, l)$ involving a mother-daughter pair of orbits of periods $p = 2^k$ and $2p = 2^{k+1}$. (b) The linking numbers $L(k, l)$ and self-linking numbers (for $k = l$) $S(k, k)$ for these orbits are related to the local torsion $T(k, k + 1)$ as indicated in this portion of the matrix of linking numbers.

$I(k, k')$		(a)	
		k	$k + 1$
k	$k + 1$	$(r_1, r_2, \dots, r_{p-1}, 0)^p$	$(r_1, r_2, \dots, r_{p-1}, r_p)^{2p}$
$k + 1$	$k + 1$	$(r_1, r_2, \dots, r_{p-1}, r_p)^{2p}$	$(r_1^2, r_2^2, \dots, r_{p-1}^2, r_p, 0)^{2p}$
		(b)	
		k	$k + 1$
k	$k + 1$	$S(k, k)$	$2 \times S(k, k) + T(k, k + 1)$
$k + 1$	$k + 1$	$2 \times S(k, k) + T(k, k + 1)$	$4 \times S(k, k) + T(k, k + 1)$

carefully for a second period-five basin. Knowing the logical sequence (xy^4) associated with the stable periodic orbit, we were able to estimate its approximate shape and location. These estimates provided initial conditions which led to rapid location of the second stable period-

five orbit. The third period-five orbit (x^3y^2) was found in the same way. Both their basins are very small. Neither had been found during earlier searches over random initial conditions in this region of the phase space, and both would have remained undiscovered without knowledge of their names (logical sequence) and this implication on orbital size and shape. The identification of the second and third period-five branches was confirmed by computing their relative rotation rates against other low periodicity orbits. These computations reproduced the intertwining matrix for the zero-torsion lift of the horseshoe map (Table IV). An additional period-five orbit has been seen experimentally.⁴⁹ Its location agrees qualitatively with the location of the second period-five orbit (x^3y^2) computed from the laser equations (2).

We expect that there are no other independent period-five branches. If additional period-five subharmonic branches were to be discovered in the laser system, they will be “snaked” to one of the three branches already discovered. The snake will be clear from its relative rotation rates. In addition, a deformation of the equations (2) can straighten out the snake, as discussed for the period-one “period-two”-branch in Sec. V. Such snakes have been observed for the period-one branch and the period-three regular saddle.

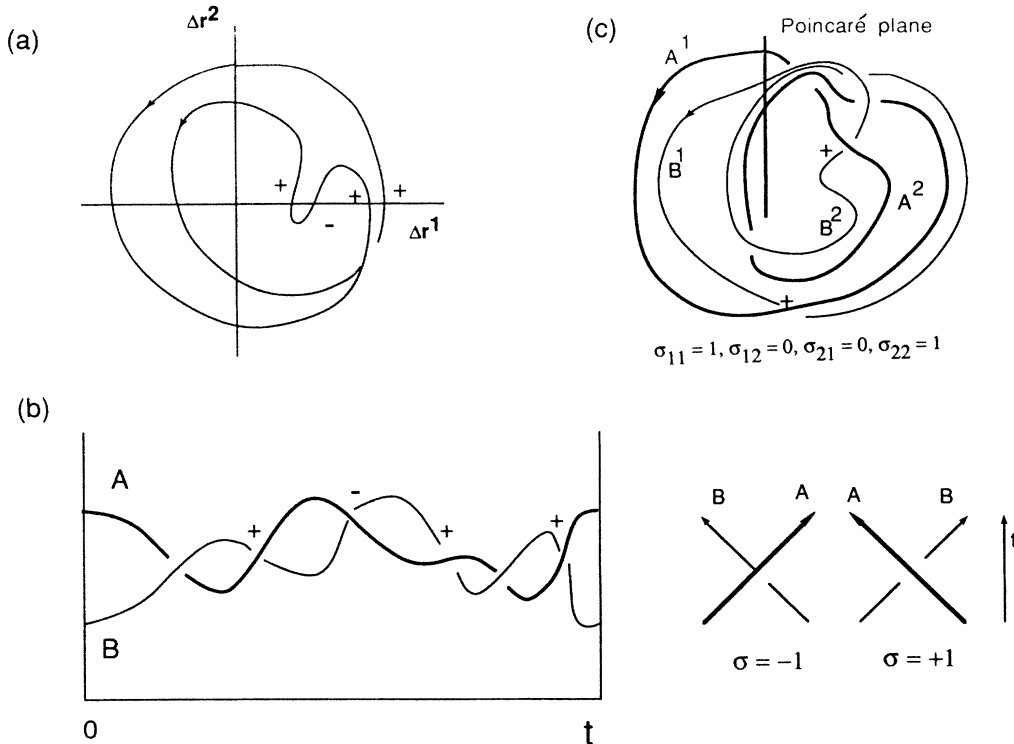


FIG. 10. The relative rotation rates of two periodic orbits are computed in three equivalent ways. (a) Each time the difference Δr crosses the half line $\Delta r^2 = 0, \Delta r^1 > 0$, the crossing direction is counted positive ($\sigma = +1$) if $d\Delta r^2/dt > 0$ and negative if $d\Delta r^2/dt < 0$. (b) Whenever A crosses over B ($\Delta r^2 = 0, \Delta r^1 > 0$), the crossing is counted positive if A crosses B from left to right (looking in the direction of the time evolution) and negative if A crosses over B from right to left. (c) Curve A is partitioned into p_A segments, A_1, A_2, \dots, A_{p_A} , where A_i connects a_i to a_{i+1} in the Poincaré plane. Curve B is treated similarly. The index σ_{ij} counts the signed number of times segment A_i crosses over segment B_j , counting $+1$ if A_i crosses over B_j from left to right and -1 if the crossing is from right to left.

VII. DISCUSSION

The relative rotation rate has been introduced as an orbit pair index with rational fractional values on pairs of periodic orbits. Their values indicate the average, per period, that one orbit winds around another. These indices are simple to measure and compute. They can even be computed for noncoexistent orbits. Their values depend on initial conditions. This definition can often be extended to noisy periodic orbits as well as strange attractors.

These indices are useful for determining whether or not two orbits can interact through bifurcation. In addition, the intertwining matrix can be used to determine the order in which bifurcations can occur. This index has been particularly useful for locating internal crises to verify the Feigenbaum ratios for the periodic and noisy periodic cascades, and the Lorenz ratio relating these cascades. It has been useful for locating boundary and external crises as well.

These dynamical indices are closely related [Eq. (5)] with topological knot-pair and knot indices, the linking and self-linking numbers. Since the dynamical indices are easily measured, the topological indices are also measurable. In fact, the dynamical index (relative rotation rate) provides more information than the topological index. In essence, this is because the topological knot is "too floppy." It can be deformed by "isotopy moves" in a way which does not preserve dynamical information, i.e., intersection with the Poincaré section. Such linking-number preserving deformations typically destroy information about the periodicity of the orbit. The relative rotation rate preserves just sufficient underlying physics (intersection with the Poincaré plane) together with the topological information (crossing numbers for return maps, see the Appendix) to summarize the physics of the flow while at the same time providing information on topological invariance.

The intertwining matrix provides information to determine a decomposition of the flow into an underlying map, which organizes the local bifurcation properties, and a lift, which determines the global flow properties. This decomposition is precise in case the map has the rigidity of a horseshoe or iterated horseshoe. The lift is then specified by a single integer, the torsion. The torsion is the relative rotation rate of the two period-one orbits.

The intertwining matrix for the laser (2) (with the snaked period-two orbits identified) and the zero-torsion lift of the horseshoe reveal that the dynamics of the laser is governed by a horseshoe. This identification has indicated that additional periodic orbits should exist. We have estimated the locations of the two additional period-five orbits in phase space (based on their "names") and their relative rotation rates with all other low period orbits. These orbits have been located where predicted and their identification has been confirmed through their relative rotation rates, which agree with the values given in Table IV.

ACKNOWLEDGMENTS

We thank K. T. Alligood, F. T. Arecchi, E. Eschenazi, C. Robinson, G. Schmidt, I. B. Schwartz, and J. R.

Tredicce for useful discussions. Support from the National Science Foundation under Grant No. PHY852-0634 is gratefully acknowledged. One of us (H.G.S.) gratefully acknowledges support from the Consejo Nacional de Investigaciones Científicas y Técnicas, Argentina.

APPENDIX: RELATIVE ROTATION RATES AND LINKING NUMBERS

In this appendix we show the relation between relative rotation rates and linking numbers. We first present three additional equivalent definitions of the relative rotation rate; from the last one the relation with the linking number is evident.

Equivalent definitions of the relative rotation rates

Let A (B) be an orbit of period p_A (p_B) which has successive intersections $[a_1, a_2, \dots, a_{p_A}]$ ($[b_1, b_2, \dots, b_{p_B}]$) with the Poincaré section. The relative rotation rates can be computed in the following four equivalent ways.

(1) The first way is

$$R_{ij}(A, B) = (1/2\pi p_A p_B) \int \mathbf{n} \cdot (\Delta \mathbf{r} \times d\Delta \mathbf{r}) / (\Delta \mathbf{r} \cdot \Delta \mathbf{r}),$$

$$\Delta \mathbf{r} = (\Delta r^1, \Delta r^2) = [x_A(t) - x_B(t), y_A(t) - y_B(t)]. \quad (\text{A1})$$

(2) Whenever $\Delta r^2 = 0$ and $\Delta r^1 \geq 0$, define $\sigma(t)$ [cf. Fig. 10(a)]

$$\sigma(t) = \begin{cases} +1 & \text{if } d\Delta r^2/dt > 0 \\ -1 & \text{if } d\Delta r^2/dt < 0. \end{cases}$$

Then

$$R_{ij}(A, B) = (1/p_A p_B) \sum_{0 \leq t \leq T_{p_A p_B}} \sigma(t). \quad (\text{A2})$$

(3) Whenever A crosses over B ($\Delta r^2 = 0$ and $\Delta r^1 > 0$), define $\sigma(t)$ by [cf. Fig. 10(b)]

$$\sigma(t) = \begin{cases} +1 & \text{if } A_i \text{ crosses } B_j \text{ from left to right} \\ -1 & \text{if } A_i \text{ crosses } B_j \text{ from right to left.} \end{cases}$$

Then

$$R_{ij}(A, B) = (1/p_A p_B) \sum_{0 \leq t \leq T_{p_A p_B}} \sigma(t). \quad (\text{A3})$$

(4) Partition the orbit A (B) into p_A (p_B) segments, each starting at a_r (b_s) and ending at the next intersection a_{r+1} (b_{s+1}). Let σ_{rs} be the number of upper crossings between the segments $(r, r+1)$ of A and $(s, s+1)$ of B . Then [cf. Fig. 10(c)]

$$R_{ij}(A, B) = (1/p_A p_B) \sum_{n=1, 2, \dots, p_A p_B} \sigma_{i+n, j+n}. \quad (\text{A4})$$

Considering the propositions 1,2,3,4 in this order, the equivalence results are self-evident.

Definitions (A2) and (A3) are more appropriate for computational purposes than the original one (A1), as they do not involve integrals. In fact, they can be implemented with an integer counter to avoid roundoff error.

Since the definition (A4) is independent of time, the entire concept of a relative rotation rate may be extended to three-dimensional autonomous dynamical systems.

The relation between relative rotation rates and linking numbers is now easily determined from (A4). In this language, the linking number is³⁷

$$L(A, B) = \sum_{A \text{ and } B} \sigma = \sum_{\substack{i,j \\ i=1, \dots, p_A \\ j=1, \dots, p_B}} \sigma_{ij} .$$

A simple manipulation of the indices gives

$$L(A, B) = \sum_{\substack{i,j \\ i=1, \dots, p_A \\ j=1, \dots, p_B}} R_{ij} , \quad (\text{A5})$$

which is the desired relation.

-
- ¹P. Cvitanovic, *Universality in Chaos* (Hilger, Bristol, 1984).
²Hao Bai-Lin, *Chaos* (World Scientific, Singapore, 1984).
³J. Guckenheimer and P. Holmes, *Nonlinear Oscillations, Dynamical Systems and Bifurcations of Vector Fields* (Springer-Verlag, New York, 1983).
⁴M. F. Bocko, D. H. Douglas, and H. H. Frutchy, *Phys. Lett.* **104A**, 388 (1984).
⁵R. van Buskirk and C. Jeffries, *Phys. Rev. A* **31**, 3332 (1985).
⁶T. Klinker, W. Meyer-Ilse, and W. Lauterborn, *Phys. Lett.* **101A**, 371 (1984).
⁷I. I. Satija, A. R. Bishop, and K. Fesser, *Phys. Lett.* **112A**, 183 (1985).
⁸F. T. Arecchi, R. Meucci, G. P. Puccioni, and J. R. Tredicce, *Phys. Rev. Lett.* **49**, 1217 (1982).
⁹R. S. Gioggia and N. B. Abraham, *Phys. Rev. Lett.* **51**, 650 (1983).
¹⁰G. P. Puccioni, A. Poggi, W. Gadomski, J. R. Tredicce, and F. T. Arecchi, *Phys. Rev. Lett.* **55**, 339 (1985).
¹¹J. R. Tredicce, F. T. Arecchi, G. L. Lippi, and G. P. Puccioni, *J. Opt. Soc. Am. B* **2**, 173 (1985).
¹²J. R. Tredicce, N. B. Abraham, G. P. Puccioni, and F. T. Arecchi, *Opt. Commun.* **55**, 131 (1985).
¹³J. R. Tredicce, F. T. Arecchi, G. P. Puccioni, A. Poggi, and W. Gadomski, *Phys. Rev. A* **34**, 2073 (1986).
¹⁴T. Midavaine, D. Dangoisse, and P. Glorieux, *Phys. Rev. Lett.* **55**, 1989 (1986).
¹⁵I. I. Matorin, A. S. Pikovskii, and Ya. I. Khanin, *Kvant. Elektron. (Moscow)* **11**, 2096 (1984) [*Sov. J. Quantum Electron.* **14**, 1401 (1984)].
¹⁶H. G. Solari, E. Eschenazi, R. Gilmore, and J. R. Tredicce, *Opt. Commun.* **64**, 49 (1987).
¹⁷F. Waldner, R. Badii, D. R. Barberis, G. Broggi, W. Floeder, P. F. Meier, R. Stoop, M. Warden, and H. Yamazaki, *J. Magn. Magn. Mater.* **54-57**, 1135 (1986).
¹⁸B. Wedding, A. Gasch, and D. Jaeger, *Phys. Lett.* **105A**, 105 (1984).
¹⁹R. Meucci, A. Poggi, F. T. Arecchi, and J. R. Tredicce (unpublished).
²⁰I. B. Schwartz and H. L. Smith, *J. Math. Biol.* **18**, 233 (1983).
²¹N. B. Tuffillaro, T. M. Mello, Y. M. Choi, and A. M. Albano, *J. Phys. (Paris)* **47**, 1477 (1986).
²²C. Robinson, *Commun. Math. Phys.* **90**, 433 (1983).
²³C. Robinson, *Trans. Am. Math. Soc.* **288**, 841 (1985).
²⁴M. J. Feigenbaum, *J. Stat. Phys.* **19**, 25 (1978).
²⁵M. J. Feigenbaum, *Los Alamos Sci.* **1**, 4 (1980).
²⁶S. Grossman and S. Thomae, *Z. Naturforsch. Teil A* **32**, 1353 (1977).
²⁷E. N. Lorenz, *Ann. N.Y. Acad. Sci.* **357**, 282 (1980).
²⁸B. A. Huberman and J. Rudnick, *Phys. Rev. Lett.* **45**, 154 (1980).
²⁹K. T. Alligood, *Trans. Am. Math. Soc.* **292**, 713 (1985).
³⁰C. Grebogi, E. Ott, and J. A. Yorke, *Physica D* **7**, 181 (1983).
³¹S. S. Chern, *J. Math. Mech.* **17**, 975 (1968).
³²J. H. White, *Am. J. Math.* **91**, 693 (1969).
³³T. Uezu and Y. Aizawa, *Prog. Theor. Phys.* **68**, 1907 (1982).
³⁴T. Uezu, *Phys. Lett.* **93A**, 161 (1983).
³⁵P. Beiersdorfer, J. M. Wersinger, and Y. Treve, *Phys. Lett.* **96A**, 296 (1983).
³⁶L. A. Santaló Sors, *Encyclopedia of Mathematics and its Applications* (Addison-Wesley, Reading, MA, 1976), Vol. 1.
³⁷D. Rolfsen, *Knots and Links* (Publish or Perish, Berkeley, CA, 1976).
³⁸J. C. Alexander and J. A. Yorke, *J. Diff. Equ.* **49**, 171 (1983).
³⁹E. N. Lorenz, *J. Atmos. Sci.* **20**, 130 (1963).
⁴⁰C. Sparrow, *The Lorenz Equations: Bifurcations, Chaos, and Strange Attractors* (Springer-Verlag, New York, 1982).
⁴¹U. Parlitz and W. Lauterborn, *Phys. Lett.* **107A**, 351 (1985).
⁴²P. Holmes, *Physica D* **21**, 7 (1986).
⁴³P. Holmes and D. Whitley, *Philos. Trans. R. Soc. London, Ser. A* **311**, 43 (1984).
⁴⁴G. Schmidt and B. W. Wang, *Phys. Rev. A* **32**, 2994 (1985).
⁴⁵J. Mallet-Paret and J. A. Yorke, *J. Diff. Equ.* **43**, 419 (1982).
⁴⁶K. T. Alligood, A. D. Yorke, and J. A. Yorke (unpublished).
⁴⁷S. Smale, *Bull. Am. Math. Soc.* **73**, 747 (1967).
⁴⁸M. Metropolis, M. L. Stein, and P. R. Stein, *J. Comb. Theory Ser. A* **15**, 25 (1973).
⁴⁹J. R. Tredicce (private communication).
⁵⁰I. Schwartz, *SIAM J. Numer. Anal.* **20**, 106 (1983).